Available online at www.sciencedirect.com
ScienceDirect
European Journal of Medicinal Chemistry 43 (2008) 2557–2567
EUROPEAN JOURNAL OF MEDICINAL CHEMISTRY
http://www.elsevier.com/locate/ejmech

Original article

A molecular model of a putative substrate releasing conformation of multidrug resistance protein 5 (MRP5)☆

Aina Westrheim Ravna, Ingebrigt Sylte*, Georg Sager

Department of Pharmacology, Institute of Medical Biology, Faculty of Medicine, University of Tromsø, MH-Building, Breivika, N-9037 Tromsø, Norway

Received 1 March 2007; received in revised form 8 October 2007; accepted 7 January 2008
Available online 25 January 2008

Abstract

The ATP-binding cassette (ABC) transporter multidrug resistance protein 5 (MRP5) contributes to the cellular export of organic anions, including guanosine 3′−5′ cyclic monophosphate (cGMP). The structural knowledge of this protein is limited, and in lack of an MRP5 X-ray structure, a model of MRP5 was constructed based on the homology with the bacterial ABC transporter Sav1866 from *Staphylococcus aureus*, which has been crystallised in an outward-facing, substrate releasing conformation. Two putative binding sites were identified, and docking of cGMP indicated that TMHs 1−3, 6, 11 and 12 were in contact with the ligands in binding site 1, while TMHs 1, 3, 5−8 were in contact with the ligands in binding site 2. The proposed MRP5 model may be used for further experimental studies of the molecular structure and function of this member of the ABC-transporter superfamily.

Keywords: MRP5; Molecular modeling; cGMP; Electrostatic potential; Ligand docking

1. Introduction

The intracellular signal molecule guanosine 3′−5′ cyclic monophosphate (cGMP) is eliminated by enzymatic conversion to GMP by cyclic nucleotide phosphodiesterases [17,18] and cellular extrusion by membrane transporters [43]. The multidrug resistance protein 5 (MRP5), also designated as ABCC5 and previously termed as MOAT-C, has been identified as a transporter for cGMP [23,51]. It has been shown that many cell types have the ability to export cGMP [43], and in agreement, MRP5 is expressed in most tissues; at the highest level in skeletal muscle, at intermediate levels in kidney, testis, heart and brain, but barely detectable in the lung and liver [5,24,33]. The protein is also localised in smooth muscle cells of the corpus cavernosum, ureter and bladder, and mucosa in ureter and urethra [37], in vascular smooth muscle cells, in cardiomyocytes, and in vascular endothelial cells in the heart [16], in brain, and capillary endothelial cells in brain, but mainly present in pyramidal neurons and astrocytes [36], and in placenta [35]. This membrane protein also identified in human erythrocytes is responsible for the high affinity transport of cGMP [23]. Immunoprecipitation of MRP5 causes a marked reduction in cGMP high affinity transport across human erythrocyte membranes [6] and the transporter discriminates in a stereo selective manner between cGMP analogues [8].

The full-length MRP5 cDNA has been cloned by several groups [5,24,47,52], but so far its 3D structure is not known. Knowledge about the 3D structure of MRP5 is important in understanding the molecular mechanisms of MRP5 mediated transport, including multidrug resistance. In order to elucidate the molecular architecture of MRP5, we have constructed a 3D molecular model of MRP5 by homology with the X-ray crystal structure of Sav1866 [15]. Homology between two proteins is determined by sequence similarity of the functional parts of

Abbreviations: ABC, ATP-binding cassette; MRP, multidrug resistance protein; NBD, nucleotide binding domain; TMD, transmembrane domain; TMH, transmembrane helix; cGMP, guanosine 3′−5′ cyclic monophosphate.

☆ Co-ordinates of the MRP5 model are available from the authors upon request.

* Corresponding author. Tel.: +47 77 64 47 05; fax: +47 77 64 53 10.
E-mail address: ingebrigt.sylte@fagmed.uit.no (I. Sylte).

0223-5234/$ - see front matter © 2008 Elsevier Masson SAS. All rights reserved.
doi:10.1016/j.ejmech.2008.01.015

two proteins having a common ancestor, which indicates the presence of similar features such as homologous protein fold. However, the amino acid composition in the binding site area may differ between protein homologues, and two homologues may bind different drugs.

MRP5 belongs to the MRP5 family of the ABC-transporter superfamily, containing four main domains in sequential order: transmembrane domain (TMD) 1, nucleotide binding domain (NBD) 1, TMD2 and NBD2, subsequently. The TMDs each contain six TMHs. The TDM0 segment of MRP1 is absent in MRP5, which gives MRP5 a P-glycoprotein-like core structure [9]. According to the functional-phylogenetic classification system for transmembrane solute transporters [44], the ABC transporters belong to category 3 (primary active transporters), subclass A (diphosphate bond hydrolysis-driven transporters) and family 1 (ABC superfamily).

Sav1866 is a homodimeric prokaryotic efflux permease featuring a total of 12 TMHs. The crystallised structure is captured in an outward-facing ATP-bound conformation [15]. The structural relationship between Sav1866 and P-glycoprotein has been confirmed [39,56], and among the ABCC transporters, MRP5 is most similar to P-glycoprotein [9], indicating that the Sav1866 X-ray crystal structure can be used as a template for constructing an MRP5 model by homology. MRP5 and P-glycoprotein are in subfamilies 3.A.208 and 3.A.201, respectively (ABC-type efflux permeases) [44], and they are closely related based on phylogeny (http://www.pasteur.fr/recherche/unites/pmtg/abc/arbre.html; with P-glycoprotein in family DPL, and MRP5 in family OAD) [11]. Phylogenetic analyses of ABC transporters have indicated that eukaryotic ABCB transporters (including P-glycoprotein), ABCC transporters (including MRP5), and bacterial ABC transporters have a common ancestor, and that they have similar domain organizations [22].

The transport cycle of ATPases follows a sequence of steps where the free energy contained within the ATP molecule is coupled to the translocation events. First, the substrate is recognised from the intracellular side, then the ATPase is stimulated and the substrate is translocated across the membrane. Finally, the substrate is released into the extracellular space. The present MRP5 model is in an outward conformation presumably representing a substrate releasing conformation. The MRP5 model was evaluated by docking of cGMP and comparing the results with site directed mutagenesis data [3,12,19,26,31,34,46,48,54].

2. Results

2.1. The MRP5 model

The energy minimized MRP5 model is shown in Fig. 1. The two TMDs form a central cavity that is open to the extracellular side and closed to the intracellular side. In this conformation, the cavity lining residues were contributed by TMHs 1–3, 5–9, 11 and 12. TMH5 of TMD1 was packed against TMH8 of TMD2 and TMH2 of TMD1 was packed against TMH11 of TMD2. The TMDs were twisted relative to the NBDs, and towards the extracellular side the TMHs diverged into two symmetrical parts, one part consisting of TMHs 1 and 2 of TMD1 and TMHs 9–12 of TMD2, and one part

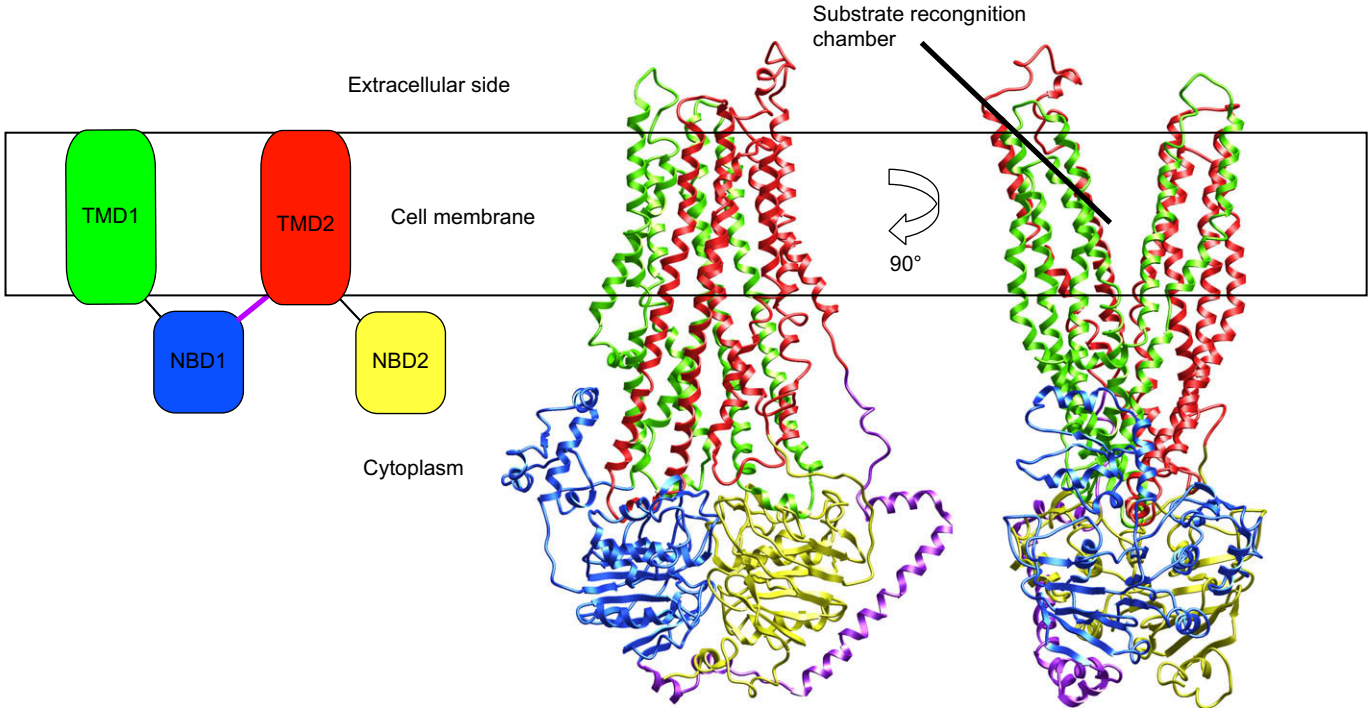

Fig. 1. Energy minimized MRP5 model viewed in the membrane plane (right), from two different views rotated 90° perpendicular to the membrane, and the corresponding MRP5 domains are schematically presented (left). The four domains of MRP5 (TMD1, green; NBD1, blue; TMD2, red; NBD2, yellow) and the loop connecting NBD1 and TMD2 (purple) are indicated in the figure.

consisting of TMHs 7 and 8 of TMD2 and TMHs 3–6 of TMD1 (Fig. 1). The loop connecting NBD1 and TMD2 of MRP5 was α-helical from residue 790 to residue 835, and in extended conformation from residue 836 to residue 848. Fig. 2 shows the EPS surface of the MRP5 model (panel A) and also a close-up of the putative substrate transport cavity (panel B). The EPS of the membrane area of the model had a dipole moment, being more positive towards the intracellular side. However, the NBD parts most distant from the membrane had areas with negative EPS (Fig. 2,panel A). As shown in panel B, the EPS of the translocation area was generally positive. Viewed from the extracellular side the substrate transport chamber was oval shaped, with a size of approximately 7 × 20 Å (Fig. 2, panel B), and closed towards the intracellular side. The two NBDs, including the nucleotide binding sites formed by the motifs Walker A, Walker B, Q-loop and switch region, were tightly packed at the intracellular side of the membrane. The two nucleotide binding sites were in direct contact at the shared interface between the NBDs. The secondary structure of the areas of each NBD forming the contact area between the two NBDs was generally in extended conformation. The interactions between the TMDs were generally hydrophobic, while the interactions between the NBDs were relatively hydrophilic.

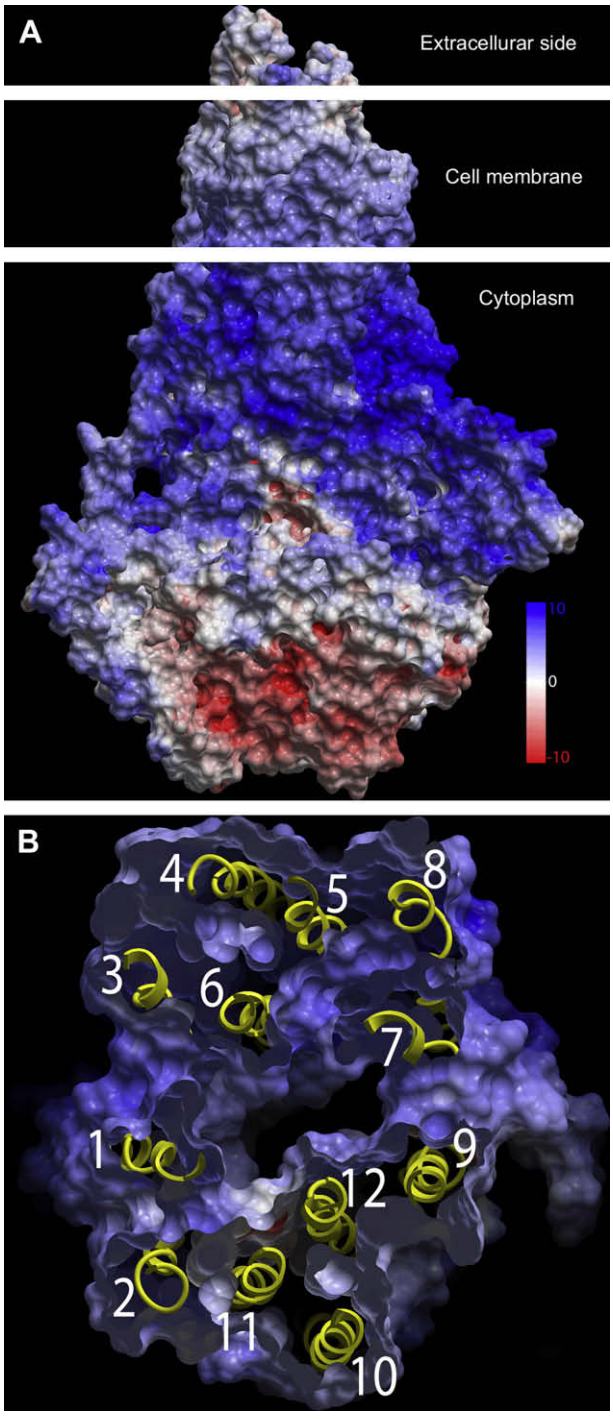

Fig. 2. The electrostatic potentials surface (EPS) of the entire MRP5 model viewed in the membrane plane (panel A), and the substrate transport chamber viewed from the extracellular side with blue areas indicating positive areas and red areas indicating negative areas. TMH numbering is indicated in white (panel B).

2.2. Validation of the model

The Errat structure validation program of the Savs Metaserver showed that the overall quality factor of the MRP5 model was 94.6. An Errat value above 90 indicates a valuable model. The Ramachandran plot provided by Procheck (Savs Metaserver) showed that 86.1% of the residues were in the most favoured regions, 11.9% were in additional allowed regions, 1.3% were in generously allowed regions, while 0.7% were in disallowed regions. The overall quality factor of the Sav1866 crystal structure was 93.6, and the Ramachandran plot showed that residues in the most favoured regions, additional allowed regions, generously allowed regions and disallowed regions were 86.0%, 14.0%, 0.0% and 0.0%, respectively. No bad contacts were reported in the MRP5 model, while 64 were reported in the Sav1866 crystal structure. The Whatcheck summary also reported that the model was satisfactory. The ProSA-web Protein Structure Analysis server reported a *Z*-score of −9.53. In comparison, the *Z*-score of the Sav1866 crystal structure is −8.29 [50]. The ProSA *Z*-score indicates the overall model quality, and *Z*-scores outside a range characteristic for native proteins indicate erroneous structures. The *Z*-scores of the MRP5 model and the Sav1866 crystal structure are in the range of experimentally determined protein chains in current PDB structures of similar sizes. The RMSD for the entire model during the last 50 ps of the molecular dynamics simulation was 1.21 Å. Altogether, these results suggested a geometrically acceptable and energetically robust model.

2.3. Binding pockets of MRP5

In the transmembrane area, two putative ligand binding pockets were predicted (Fig. 3). Pocket 1 involved TMHs 1 and 2 of TMD1 and TMHs11 and 12 of TMD2, while Pocket 2 involved TMHs 5 and 6 of TMD1 and TMHs 7 and 8 of TMD2. Each predicted pocket contained one positively charged amino acid; Arg232 (TMH2) in Binding Pocket 1

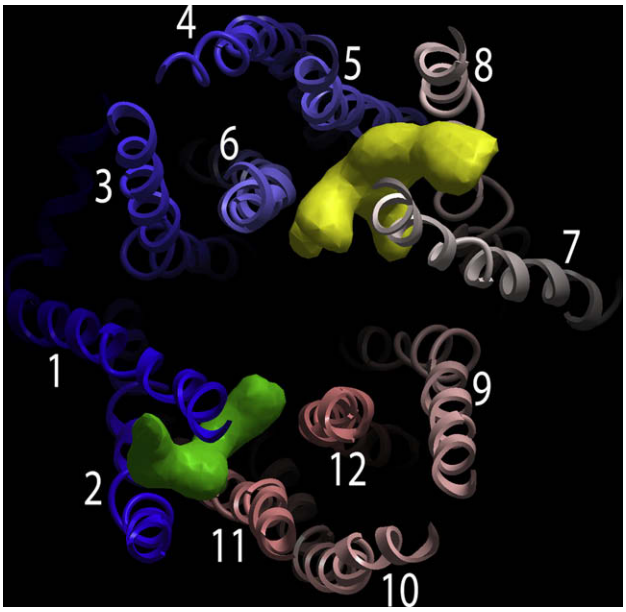

Fig. 3. The binding cavities in the transmembrane area of the MRP5 model, viewed from the extracellular side, as characterized by ICM Pocket Finder. Binding Pocket 1 is shown in green and Binding Pocket 2 is shown in yellow. The C_α-traces of MRP5 are shown with colour codes of the sequence order; from blue (N-terminal) to red (C-terminal).

and Lys448 (TMH6) in Binding Pocket 2. The amino acids surrounding the predicted binding pockets are listed in Table 1. Both Arg232 and Lys448 were considered as possible recognition points for organic anions.

2.4. cGMP–MRP5 interactions

Docking of cGMP into the two putative binding sites of MRP5's transport chamber is shown in Fig. 4 (panels A and B). Twenty-five docking poses were sampled and compared in both binding pockets. MRP5 amino acid residues in contact with cGMP during the automatic interactive docking procedures are shown in Table 1. Altogether 42 amino acids were reported as putative cGMP binding amino acids (Table 1); 21 localised in Binding Pocket 1 (TMHs 1–4, 11 and 12), and 25 localised in Binding Pocket 2 (TMHs 1, 3, 5–8). In Binding Pocket 1, the negatively charged phosphate group of cGMP formed a salt bridge with Arg232 in most of the 25 poses reported by ICM. In the different docking poses, the purine base of cGMP interacted with Gln190 or Gln1144. In Binding Pocket 2 several of the 25 docking poses of cGMP sampled during the ICM automatic docking suggested a salt bridge between the negatively charged phosphate group of cGMP and Lys448 (TMH6), while the purine base of cGMP had contact with Phe445 and Asn441 (TMH6). During the docking sessions, cGMP in general had contact with the amino acids proposed by the ICM Pocket Finder to be involved in the binding pockets (Table 1). In addition, Binding Pocket 1 also involved TMHs 3 and 6, while Binding Pocket 2 involved TMHs 1 and 3. The binding sites were slightly overlapping; Gln190 and Gly193 (TMH1), Leu297 (TMH3) and Phe445

Table 1
Amino acid residues surrounding Binding Pockets 1 and 2 predicted by ICM Pocket Finder (column 2), and amino acid residues in contact with cGMP in the two interactive docking sessions (column 3)

TMH	Binding Pocket 1		Binding Pocket 2	
	Predicted by the ICM Pocket Finder	Docking	Predicted by the ICM Pocket Finder	Docking
1		Leu186		
		Thr189		
		Gln190		Gln190
	Ala192	Ala192		
	Gly193	Gly193		Gly193
	Ser195	Ser195		
	Gly196	Gly196		
	Pro197	Pro197		
	Phe199			
2	Gly224			
	Thr228			
	Arg232	Arg232		
		Leu236		
		Trp240		
3		Leu297		Leu297
				Pro301
				Ala304
5				Val403
				Pro407
			Val411	Val411
			Ser414	Ser414
				Phe418
6			Phe440	Phe440
			Asn441	Asn441
			Thr444	Thr444
		Phe445	Phe445	Phe445
			Lys448	Lys448
				Phe452
7				Val861
			Ala864	
			Leu865	Leu865
			Met867	
			Leu868	Leu868
				Val870
			Gly871	Gly871
			Ser872	Ser872
			Ala874	
			Phe875	Phe875
			Trp879	
8			Ala919	
			Ala923	
			Ile927	Ile927
			Ile931	Ile931
11		Ala1099		
		Asp1103		
	Ile1107	Ile1107		
	Ile1110	Ile1110		
12	Val1137	Val1137		
	Thr1140	Thr1140		
	Gln1144	Gln1144		
		Val1147		

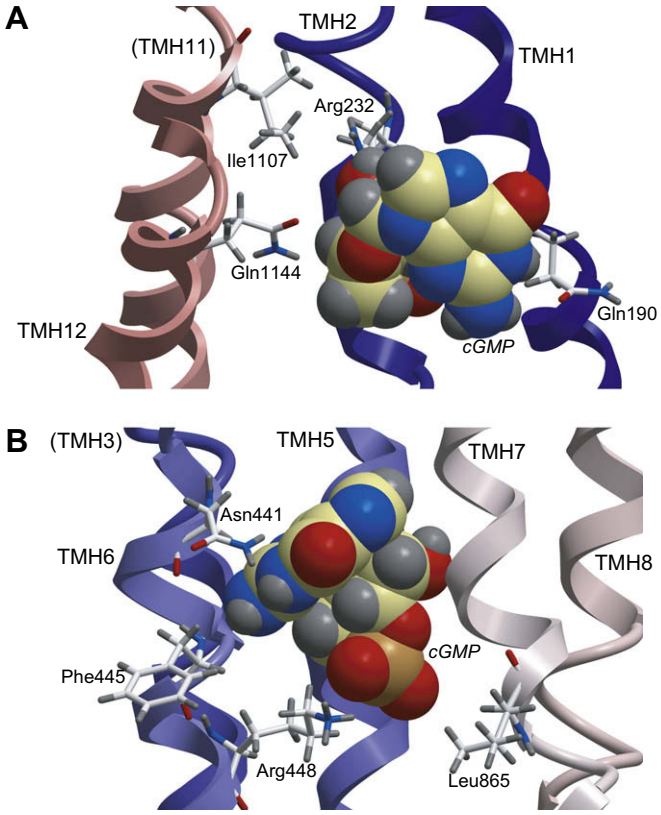

Fig. 4. It has been shown that cGMP is transported by MRP5 with high affinity [23]. The docking of cGMP into Binding Pocket 1 (panel A) and into Binding Pocket 2 (panel B) of the MRP5 model is viewed in the membrane plane. Displayed amino acids interacting with the ligands are Gln190 (TMH1), Arg232 (TMH2), Ile1107 (TMH11) and Gln1144 (TMH12) (panel A), and Asn441, Phe445 and Lys448 (TMH6) and Leu865 (TMH7) (panel B). The different atoms are indicated as follows: carbon, oxygen, nitrogen, phosphor and hydrogen with yellow, red, blue, orange and grey, respectively. The C_α-traces of MRP5 are shown with colour codes of the sequence order; from blue (N-terminal) to red (C-terminal). TMHs that are located behind a TMH are indicated in parentheses.

(TMH6) had contact with cGMP in docking poses from both docking sessions.

3. Discussion

Among the members of the ABC-transporter family, MRP5 has been shown to transport cGMP with high affinity [23]. It has been possible to restore ATP-dependent cGMP transport into proteoliposomes by membrane proteins from human erythrocytes [6,7] and cGMP-induced ATPase activity [7]. However, our attempts to isolate and purify MRP5 in a yield and quality for X-ray crystallographic studies have failed so far. The present study contributes with hypotheses about the 3D structure and cGMP binding of MRP5, and was performed awaiting a MRP5 crystal structure of MRP5. The proposed model, representing an outward-facing conformation, indicated that two putative cGMP binding sites are formed, Binding Pocket 1 including TMHs 1–3, 6, 11, and 12, and Binding Pocket 2 including TMHs 1, 3, 5–8. According to the intractive docking session, these binding sites are slightly overlapping. Based on knowledge from other protein families, a possible cGMP binding site could also have been located at the interface between the half-transporters, since substrate binding might require residues from both predicted pockets. However, the ICM Pocket Finder did not report a putative binding site in this region, but reported two distinct, but close, binding sites, and cGMP was docked into each of the two predicted binding pockets in two separate docking sessions. The presence of several binding sites is in accordance with experimental studies on other multidrug resistance transporters, such as MRP4 [49]. However, the two binding pockets were predicted from an outward-facing conformation. The presence of two or more binding sites in a substrate recognition conformation remains to be confirmed.

Cyclic GMP binds to a high affinity binding site accessible to the intracellular side of MRP5. During the translocation process the binding site changes conformation, and cGMP is released to the extracellular side from a low affinity binding site. The present MRP5 model is assumed to be in a conformation representing the last event, thus cGMP presumably binds to the present MRP5 model with a low affinity. But even though the Sav1866 structure is captured in an outward-facing and probably low affinity conformation of the protein and does not represent the best suitable template for modeling a high affinity cGMP binding site, the amino acids in the binding sites predicted by ICM Pocket Finder, and those suggested by the interactive docking sessions (Table 1), may give hypotheses about amino acids involved in substrate recognition and binding during translocation. Therefore the present molecular modeling study contributes with predictions for further experimental studies by protein engineering experiments. However, the present model should not be used to correlate calculated binding energies of the docking complexes with experimental values for cGMP binding affinity to MRP5, since such binding affinity values reflect binding affinity in the high affinity, inward facing conformation of the binding site. Therefore, binding energies of the docking complexes were not calculated.

MRP5 is classified as an anion-transporter since non-selective anion transport inhibitors (such as probenecid and sulfinpyrazone) reduce substrate translocation [38,40,51,52]. In agreement, the present model shows that the transport chamber was generally positively charged. The attraction between the negatively charged anions and the positively charged transport chamber may thus be the first step in the sequence of events leading to translocation.

Interactions between glutamine and phenylalanine residues and the purine group of cGMP are seen in the crystal structure of cGMP specific phosphodiesterase, PDE5A [55]. In the present docking studies, similar interactions are seen between the purine group of cGMP and Gln190 (TMH1) and Gln1144 (TMH12) (Binding Pocket 1), and Phe445 and Asn441 (TMH6) (Binding Pocket 2). Site directed mutagenesis studies, photolabeling studies and molecular modeling studies of MRP1 indicated that interactions involving residues in TMH11 influence the substrate specificity of MRP1 [12,53]. TMH11 in MRP1 corresponds to TMH6 in MRP5, since MRP1 has five TMHs in its TMD0. The functional importance

of the MRP1 residue Phe594 [12], corresponding to Phe445 in MRP5, and the involvement of MRP1 residues Asn590, Arg593 and Asn597 [53], corresponding to Asn441, Thr444 and Lys448 in MRP5, respectively, support the model of MRP5 and its interaction with cGMP. Structure–function investigations of the cystic fibrosis transmembrane conductance regulator (CFTR) also indicate that its TMH6 plays a central role in forming the pore and determining its functional properties [19]. More specifically, Arg334 [46], Lys335 [3,48], Ser341 [34] and Arg347 [48] may contribute to the control of Cl^- permeation, directly or indirectly [19]. Several cross-linking and site directed mutagenesis data have been published for P-glycoprotein supporting the 3D architecture of the MRP5 model [26–32]. In agreement with the present model, these studies indicated that TMH6 and TMH12 are involved in ligand binding [26,30–32]. Cross-linking has shown that TMH5 and TMH8 are close to each other [27], and that TMH2 and TMH11 are close to each other [28]. As shown in Fig. 4, these experimental data are consistent with the helical architecture of the present MRP5 model. Site directed mutagenesis studies on P-glycoprotein have proposed a verapamil binding site that includes Leu65 (TMH1) [32], Ile306 (TMH5) [32], Ile340 (TMH6) [10,32] and Phe343 (TMH6) [31]. The corresponding residues in MRP5 are Gln190 (TMH1), Val410 (TMH5), Asn441 (TMH6) and Thr444 (TMH6). Gln190 (TMH1), Asn441 (TMH6) and Thr444 (TMH6) were all in contact with cGMP (Table 1). A sequence alignment of TMH6 of MRP5, MRP1, CFTR and P-glycoprotein is shown in Fig. 5, indicating amino acids interacting with ligands in the present MRP5 docking studies, together with amino acids shown to interact with ligands in site directed mutagenesis studies on MRP1, CFTR and P-glycoprotein.

It is believed that quite accurate structure predictions can be made with an amino acid sequence similarity greater than 50% between the target and the template protein. Also relevant is the conservation and length of the secondary structure elements. However, even with overall sequence similarities less than 15% there may be considerable structural similarities within highly conserved regions. The sequence similarities within the transmembrane regions between G-protein coupled receptors (GPCR) and bacteriorhodopsin are only 6–11% [20] and nevertheless they share an overall common folding pattern. The sequence identity between the target molecule MRP5 and the template molecule Sav1866 is ~23%. The identities between the Sav1866 TMD and the MRP5 TMD1 and TMD2 are 21% and 14%, respectively. In comparison, the identity between the MRP5 TMD1 and TMD2 is 15%. The length of the Sav1866 TMD is 284 amino acids, while the lengths of the MRP5 TMD1 and TMD2 are 275 and 294 amino acids, respectively. At present, it seems that the Sav1866 X-ray structure is the only suitable template for MRP5 modeling. A conformation open to the intracellular side is considered as more representative for the high affinity ligand binding and may be more suitable for investigating high affinity ligand recognition. From a pharmacological point of view, the specificity and affinity of MRP5 substrate binding are of particular interest since various drugs and endogenous substances are MRP5 substrates [41]. For this reason, focus was kept on the TMH area, and not the NBDs, of the MRP5 model. It has been reported that the two NBDs of CFTR are not functionally equivalent, with both NBDs involved in ATP binding whereas only one NBD is responsible for ATP hydrolysis, while for ABCB1, both NBDs are responsible for ATP binding and hydrolysis [45]. The NBDs of Sav1866 are also functionally equivalent [15]. For MRP5 it has not been reported whether its NBDs are functionally equivalent or not, so in this aspect it is uncertain whether the NDBs of Sav1866 are representative templates for modeling the MRP5 NBDs.

Even though the overall fold of the MRP5 model may be realistic, the low sequence identity (23%) between MRP5 and the template protein indicates structural differences in less conserved regions. Most probably, the template used for the modeling also represents a low affinity conformation. Detailed conclusions regarding side-chain positions, helical packing and cGMP binding are therefore not possible. But the docking results may still give hypotheses about the interactions of cGMP with the MRP5 binding site at the molecular level. However, we feel that the relatively low homology between the model and the template, and the uncertainties connected to each step in the modeling procedure, contributes to a level of molecular accuracy not good enough for detailed calculations of the free energy of ligand binding. For the same reason, water molecules and membrane phospholipids were also not included in the modeling. Solvation and membrane molecules would have complicated the model and contributed with even more uncertainties. The omission of C- and N-terminals should also be kept in mind when interpreting the overall EPS of the MRP5 model. However, the TMD part oriented towards cytoplasm is more positive than the TMD part oriented towards the extracellular side, supporting the "positive inside rule" of membrane proteins. Intriguingly, the NBD parts farther into the cytoplasm had areas with negative EPS, indicating that intracellular organic anions are repelled from the transporter in the present conformation.

In general, X-ray crystallography and NMR techniques are used for structural determination of proteins at an atomic

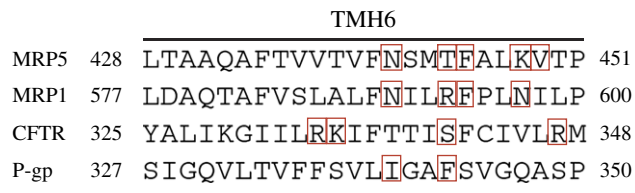

Fig. 5. Sequence alignment of TMH6 of MRP5, MRP1, CFTR and P-glycoprotein (P-gp). Red boxes indicate amino acids interacting with ligands in the present docking studies (MRP5) and amino acids shown to interact with ligands in site directed mutagenesis studies (MRP1, CFTR and P-glycoprotein). Boxed amino acids are as follows: MRP5: Asn441, Thr444, Phe445, Lys448 and Val 449; MRP1: Asn590 [54], Arg593 [54], Phe594 [12] and Asn597 [54]; CFTR: Arg334 [46], Lys335 [3,48], Ser341 [34] and Arg347 [48]; P-glycoprotein: Ile340 [31] and Phe343 [26]. (For interpretation of the references to colour in this figure legend, the reader is referred to the web version of this article.)

resolution, but making crystals of membrane proteins is technically difficult, and molecular modeling might be used as a step forward towards structural knowledge of drug targets when no experimental structure is available. The MRP5 model presented is mainly considered as a preliminary working tool for generating hypotheses and designing further experimental studies related to ABC-transporter structure and function and their ligand interactions. In this study, we suggest 42 amino acids as possible candidates for single point mutations (Table 1). Site directed mutagenesis studies and ABC-transporter modeling are complementary to each other in an iterating process towards a better understanding of the structure and function of these proteins. The results from the present docking studies were in accordance with experimental data, which indicate that the Sav1866 X-ray structure [15] may serve as a suitable template for MRP5 modeling. The docking studies in this modeling study were performed in order to elucidate amino acids in the MRP5 binding site area that may be mutated in site directed mutagenesis studies. Specifically, the hypothesis suggesting that a binding pocket for organic anions is localised along TMH6 can be investigated by mutating Asn441, Thr444, Phe445 and Lys448 of MRP5 and observe whether cGMP binding is affected. The present modeling study may be used as a general tool for designing experimental studies on MRP5. Knowledge about ABC-transporter structure can be used to develop membrane transport modulating agents, which, in turn, can be helpful to overcome multidrug resistance.

4. Materials and methods

4.1. Modeling procedure

Multiple sequence alignments of human MRP5 (SWISS-PROT accession number O15440), human MRP8 (SWISS-PROT accession number Q9BX80), human MRP4 (SWISS-PROT accession number O15439), human P-glycoprotein /MDR1 (SWISS-PROT accession number P08183), Sav1866 (SWISS-PROT accession number Q99T13), *Vibrio cholerae* MsbA (SWISS-PROT accession number Q9KQW9) and *Escherichia coli* MsbA (SWISS-PROT accession number P60752) were performed using T-COFFEE, Version 4.71 available at the Le Centre national de la recherche scientifique website (http://www.igs.cnrs-mrs.fr/Tcoffee/tcoffee_cgi/index.cgi) and the ICM software Version 3.4-4 [2]. Predictions of start- and endpoints of MRP5 TMHs were obtained from the PredictProtein server for sequence analysis and structure prediction [42], and SWISS-PROT [4]. The start- and endpoints of the TMHs of Sav1866 and the predicted start- and endpoints of the TMHs of MRP5 (Table 2) were located at similar positions in the T-COFFEE and ICM alignments, indicating that the alignments could serve as guidelines for the homology modeling process.

Version 3.4-4 of the ICM software [2] was used for homology modeling and ligand docking. The ICM program performs homology modeling by constructing the model from a few core sections defined by the average of C_α atom positions in the conserved regions. The X-ray structure of Sav1866 (PDB code 2HYD) [15] from *Staphylococcus aureus* was used as a template to construct a model of the MRP5 transporter using the homology modeling module of the ICM program, which also constructs loops [1]. The fast loop "placement" option of ICM was used, which searches for loops matching in regard to sequence similarity and sterical interactions with the surroundings of the model, within several thousand high quality PDBs. The maps around are calculated and the loops are scored based on their relative energies, selecting the best fitting one. The amino acids in the loop connecting NBD1 and TMD2 of MRP5, amino acids 778–848, were also included in this modeling step. The Sav1866 and human MRP5 amino acid sequences were manually adjusted based on the multiple T-COFFEE and ICM alignments, and the information from the PredictProtein server [42] and SWISS-PROT [4] about predicted start- and endpoints of the MRP5 TMHs, and used as input for the homology modeling by the ICM program. The resulting start- and endpoints of the MRP5 TMHs after manual adjustment are shown in Table 2. The input alignment for the modeling procedure is shown in Fig. 6. N- and C-terminals were not included in the modeling procedure.

Table 2
Sav1866 TMH start- and endpoints and the predicted start- and endpoints of the TMHs of MRP5 compared with amino acid positions of MRP5 and Sav1866 amino acid sequences in the T-COFFEE alignment

Segment	MRP5 TMHs (SWISS-PROT)		MRP5 TMHs (the PredictProtein server)		Sav1866 X-ray structure TMHs [14]		MRP5 TMHs according to Sav1866 X-ray and T-COFFEE alignment	
	Start	End	Start	End	Start	End	Start	End
TMH1	179	199	174	192	14	39	177	202
TMH2	219	239	219	236	56	82	214	240
TMH3	296	316	300	324	138	159	294	315
TMH4	317	337	329	346	162	188	318	343
TMH5	400	420	403	420	247	268	402	423
TMH6	434	454	430	447	275	298	428	451
TMH7	848	868	856	873	14	39	852	882
TMH8	917	937	917	934	56	82	909	935
TMH9	997	1017	996	1020	138	159	989	1010
TMH10	1018	1038			162	188	1013	1039
TMH11	1104	1124	1095	1117	247	268	1098	1119
TMH12	1127	1147	1123	1140	275	298	1124	1147

The MRP5 model was energy refined using the refineModel macro of ICM. This macro includes (1) a Monte Carlo simulation [1] of side chains, (2) five steps of iterative annealing of backbone, and (3) a second Monte Carlo simulation of side chains. During the ICM energy minimization restraints were used to keep the backbone atoms at the same positions as in the template. The refined MRP5 model was subjected to two subsequent energy minimizations by the AMBER 8.0 program package, using the leaprc.ff03 force field [13]. The first energy minimization by the AMBER 8.0 program package was performed with restrained backbone by 500 cycles of the steepest descent minimization followed by 500 steps of conjugate gradient minimization. The second energy minimization was

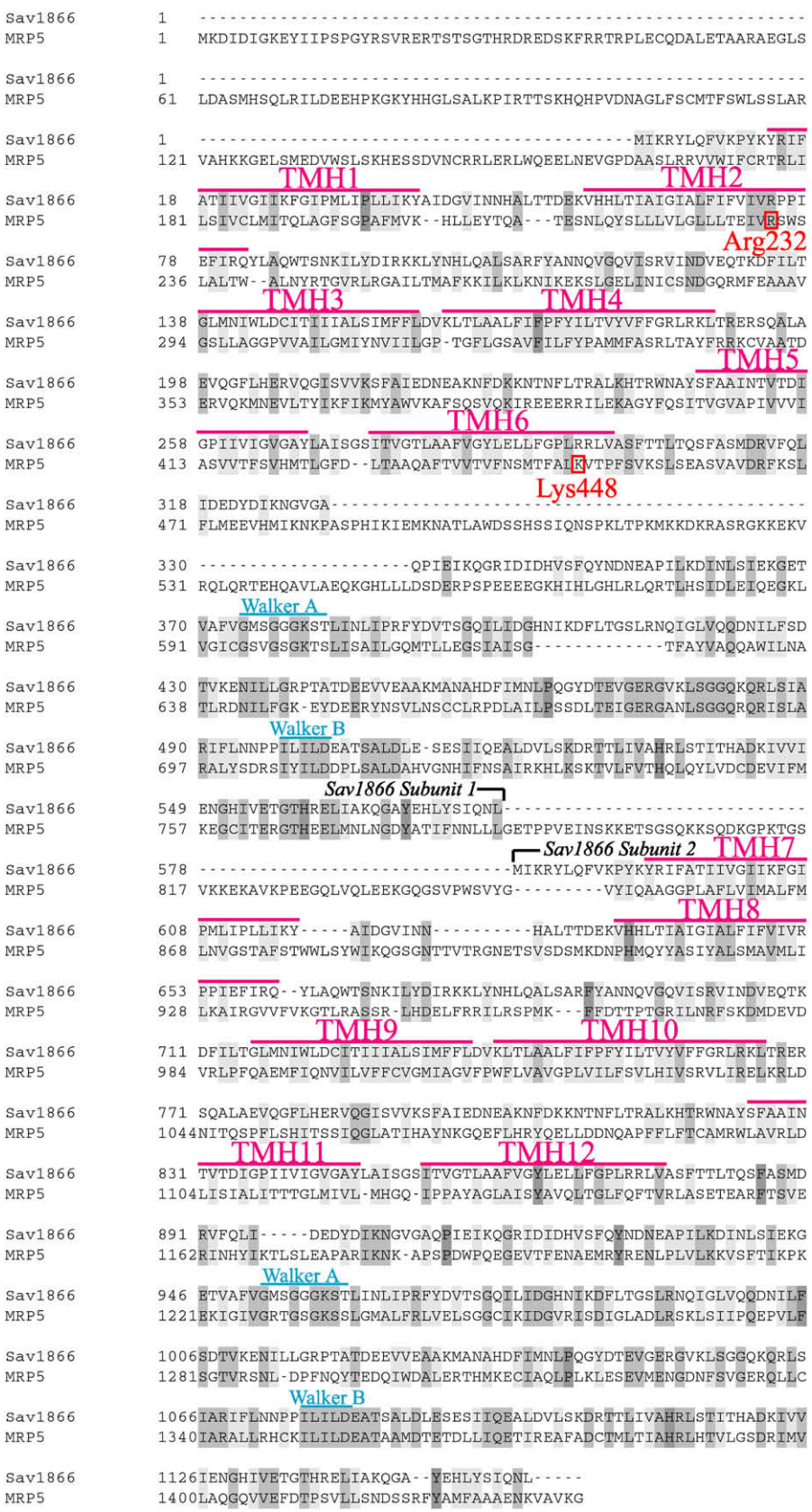

Fig. 6. Pairwise amino acid sequence alignment of MRP5 and Sav1866. TMHs (magenta) and Walker motifs (cyan) are indicated in the figure. The positions of Arg232 and Lys488 in the alignment are indicated in red. Colour coding between aligned sequences: identical: darker grey, similar: lighter grey. (For interpretation of the references to colour in this figure legend, the reader is referred to the web version of this article.)

performed with no restraints by 1000 cycles of the steepest descent minimization followed by 1500 steps of conjugate gradient minimization. A 10 Å cut-off radius for nonbonded interactions and a dielectric multiplicative constant of 1.0 for the electrostatic interactions were used in the molecular mechanics calculations. The electrostatic potential surface (EPS) of the MRP5 model was also calculated with the ICM program. In order to check the robustness of the model, it was subjected to 80 ps of molecular dynamics with gradual heating (0–300 K) during the first 30 ps and a constant temperature of 300 K during the remaining 50 ps. The AMBER 8.0 program was used for the molecular dynamics simulations, and water molecules were not included. The conformations after 30 ps and 80 ps of molecular dynamics were energy minimized, and the RMSD relative to the structure before molecular dynamics was calculated for the co-ordinates obtained every 5 ps during the last 50 ps of the molecular dynamics simulations using the ptraj program of the AMBER 8.0 program.

4.2. Validation of the model

The Procheck [25], Whatcheck [21] and Errat [14] programs of the Savs Metaserver for analyzing and validating protein structures (http://nihserver.mbi.ucla.edu/SAVS/), and the ProSA-web Protein Structure Analysis server (https://prosa.services.came.sbg.ac.at/prosa.php) [50], were used to check the stereochemical quality of the MRP5 model.

4.3. Ligand molecules

The chemical structure of cGMP was employed in the study. The crystal structure of cGMP was used as input PDB structure for the Leap and Antechamber programs of the AMBER 8.0 program package [13]. The X-windows graphical interface of the xleap shell scripts and the Antechamber program was used to assign atomic charges and atom types of cGMP. The Sander program of the AMBER 8.0 program package was used for energy minimization of the cGMP molecule using the leaprc.gaff force field.

4.4. Ligand docking

The X-ray crystal structures of two cGMP–protein complexes were used to assign possible binding modes of cGMP to the putative substrate releasing conformation of MRP5. In the X-ray crystal structure of the C-terminal fragment of hyperpolarization-activated, cyclic nucleotide modulated channel 2 with cGMP, a salt bridge is seen between the phosphate group of cGMP and an arginine residue [53]. In the X-ray crystal structure complex of cyclic nucleotide phosphodiesterase 5A and GMP [55] the purine group of GMP interacts with glutamine and phenylalanine residues.

Possible ligand binding cavities of the MRP5 model were identified using ICM Pocket Finder, which detects cavities of sufficient size to bind ligands. The tolerance level used was 4.6, thus cavities with a volume greater than 4.6 $Å^3$ were considered. The ICM Pocket Finder indicated that Lys448 in TMH6 is within one possible binding pocket, and Arg232 in TMH2 where in another possible binding pocket. It was therefore anticipated that Lys448 and Arg232 could be ligand anchoring points in MRP5 similar to the arginine in the hyperpolarization-activated, cyclic nucleotide modulated channel (HCN2) [53]. Lys448 and Arg232 were therefore the ligand anchoring points during two ICM interactive docking procedures of cGMP. The ICM ligand docking procedure performs docking of the fully flexible small-molecule ligand to the drug target model, and contributes to prediction of correct binding geometry for the ligand. The global minimum of the energy function, which includes description of the interaction of the flexible ligand with the receptor and the internal conformational energy of the ligand, is calculated via an ICM stochastic global optimization algorithm. During an interactive docking session a stack of alternative low energy conformations is saved.

Acknowledgements

This work has been supported with grants from The Norwegian Cancer Society.

References

[1] R. Abagyan, M. Totrov, Biased probability Monte Carlo conformational searches and electrostatic calculations for peptides and proteins, J. Mol. Biol. 235 (1994) 983–1002.
[2] R. Abagyan, M. Totrov, D.N. Kuznetsov, ICM – a new method for protein modeling and design. Applications to docking and structure prediction from the distorted native conformation, J. Comput. Chem. 15 (1994) 488–506.
[3] M.P. Anderson, R.J. Gregory, S. Thompson, D.W. Souza, S. Paul, R.C. Mulligan, A.E. Smith, M.J. Welsh, Demonstration that CFTR is a chloride channel by alteration of its anion selectivity, Science 253 (1991) 202–205.
[4] A. Bairoch, R. Apweiler, The SWISS-PROT protein sequence data bank and its supplement TrEMBL in 1999, Nucleic Acids Res. 27 (1999) 49–54.
[5] M.G. Belinsky, L.J. Bain, B.B. Balsara, J.R. Testa, G.D. Kruh, Characterization of MOAT-C and MOAT-D, new members of the MRP/cMOAT subfamily of transporter proteins, J. Natl. Cancer Inst. 90 (1998) 1735–1741.
[6] E. Boadu, G. Sager, Reconstitution of ATP-dependent cGMP transport into proteoliposomes by membrane proteins from human erythrocytes, Scand. J. Clin. Lab. Investig. 64 (2004) 41–48.
[7] E. Boadu, G. Sager, ATPase activity and transport by a cGMP transporter in human erythrocyte ghosts and proteoliposome reconstituted membrane extracts, Biochim. Biophys. Acta 1509 (2000) 467–474.
[8] E. Boadu, S. Vaskinn, E. Sundkvist, R. Jaeger, G. Sager, Inhibition by guanosine cyclic monophosphate (cGMP) analogues of uptake of [^{3}H]3′,5′-cGMP without stimulation of ATPase activity in human erythrocyte inside-out vesicles, Biochem. Pharmacol. 62 (2001) 425–429.
[9] P. Borst, R. Evers, M. Kool, J. Wijnholds, The multidrug resistance protein family, Biochim. Biophys. Acta 1461 (1999) 347–357.
[10] P. Borst, R. Evers, M. Kool, J. Wijnholds, A family of drug transporters: the multidrug resistance-associated proteins, J. Natl. Cancer Inst. 92 (2000) 1295–1302.
[11] P. Bouige, D. Laurent, L. Piloyan, E. Dassa, Phylogenetic and functional classification of ATP-binding cassette (ABC) systems, Curr. Protein Pept. Sci. 3 (2002) 541–559.

[12] J.D. Campbell, K. Koike, C. Moreau, M.S. Sansom, R.G. Deeley, S.P. Cole, Molecular modeling correctly predicts the functional importance of Phe594 in transmembrane helix 11 of the multidrug resistance protein, MRP1 (ABCC1), J. Biol. Chem. 279 (2004) 463–468.
[13] D.A. Case, T.A. Darden, T.E. Cheatham III, C.L. Simmerling, J. Wang, R.E. Duke, R. Luo, K.M. Merz, B. Wang, D.A. Pearlman, M. Crowley, S. Brozell, V. Tsui, H. Gohlke, J. Mongan, V. Hornak, G. Cui, P. Beroza, C. Schafenmeister, J.W. Caldwell, W.S. Ross, P.A. Kollman, AMBER 8, University of California, San Francisco, 2004.
[14] C. Colovos, T.O. Yeates, Verification of protein structures: patterns of nonbonded atomic interactions, Protein Sci. 2 (1993) 1511–1519.
[15] R.J.P. Dawson, K.P. Locher, Structure of a bacterial multidrug ABC transporter, Nature 443 (2006) 180–185.
[16] P. Dazert, K. Meissner, S. Vogelgesang, B. Heydrich, L. Eckel, M. Bohm, R. Warzok, R. Kerb, U. Brinkmann, E. Schaeffeler, M. Schwab, I. Cascorbi, G. Jedlitschky, H.K. Kroemer, Expression and localization of the multidrug resistance protein 5 (MRP5/ABCC5), a cellular export pump for cyclic nucleotides, in human heart, Am. J. Pathol. 163 (2003) 1567–1577.
[17] S.H. Francis, M.A. Blount, R. Zoraghi, J.D. Corbin, Molecular properties of mammalian proteins that interact with cGMP: protein kinases, cation channels, phosphodiesterases, and multi-drug anion transporters, Front. Biosci. 10 (2005) 2097–2117.
[18] S.H. Francis, I.V. Turko, J.D. Corbin, Cyclic nucleotide phosphodiesterases: relating structure and function, Prog. Nucleic Acid Res. Mol. Biol. 65 (2001) 1–52.
[19] A. Frelet, M. Klein, Insight in eukaryotic ABC transporter function by mutation analysis, FEBS Lett. 580 (2006) 1064–1084.
[20] M.F. Hibert, S. Trumpp-Kallmeyer, A. Bruinvels, J. Hoflack, Three-dimensional models of neurotransmitter G-binding protein-coupled receptors, Mol. Pharmacol. (1991) 8–15.
[21] R.W. Hooft, G. Vriend, C. Sander, E.E. Abola, Errors in protein structures, Nature 381 (1996) 272.
[22] Y. Igarashi, K.F. Aoki, H. Mamitsuka, K. Kuma, M. Kanehisa, The evolutionary repertoires of the eukaryotic-type ABC transporters in terms of the phylogeny of ATP-binding domains in eukaryotes and prokaryotes, Mol. Biol. Evol. 21 (2004) 2149–2160.
[23] G. Jedlitschky, B. Burchell, D. Keppler, The multidrug resistance protein 5 functions as an ATP-dependent export pump for cyclic nucleotides, J. Biol. Chem. 275 (2000) 30069–30074.
[24] M. Kool, M. de Haas, G.L. Scheffer, R.J. Scheper, M.J. van Eijk, J.A. Juijn, F. Baas, P. Borst, Analysis of expression of cMOAT (MRP2), MRP3, MRP4, and MRP5, homologues of the multidrug resistance-associated protein gene (MRP1), in human cancer cell lines, Cancer Res. 57 (1997) 3537–3547.
[25] R.A. Laskowski, D.S. Moss, J.M. Thornton, Main-chain bond lengths and bond angles in protein structures, J. Mol. Biol. 231 (1993) 1049–1067.
[26] T.W. Loo, M.C. Bartlett, D.M. Clarke, Methanethiosulfonate derivatives of rhodamine and verapamil activate human P-glycoprotein at different sites, J. Biol. Chem. 278 (2003) 50136–50141.
[27] T.W. Loo, M.C. Bartlett, D.M. Clarke, Disulfide cross-linking analysis shows that transmembrane segments 5 and 8 of human P-glycoprotein are close together on the cytoplasmic side of the membrane, J. Biol. Chem. 279 (2004) 7692–7697.
[28] T.W. Loo, M.C. Bartlett, D.M. Clarke, Val133 and Cys137 in transmembrane segment 2 are close to Arg935 and Gly939 in transmembrane segment 11 of human P-glycoprotein, J. Biol. Chem. 279 (2004) 18232–18238.
[29] T.W. Loo, M.C. Bartlett, D.M. Clarke, Transmembrane segment 7 of human P-glycoprotein forms part of the drug-binding pocket, Biochem. J. 399 (2006) 351–359.
[30] T.W. Loo, M.C. Bartlett, D.M. Clarke, Transmembrane segment 1 of human P-glycoprotein contributes to the drug binding pocket, Biochem. J. 396 (2006) 537–545.
[31] T.W. Loo, D.M. Clarke, Location of the rhodamine-binding site in the human multidrug resistance P-glycoprotein, J. Biol. Chem. 277 (2002) 44332–44338.
[32] T.W. Loo, D.M. Clarke, Recent progress in understanding the mechanism of P-glycoprotein-mediated drug efflux, J. Membr. Biol. 206 (2005) 173–185.
[33] M.A. McAleer, M.A. Breen, N.L. White, N. Matthews, pABC11 (also known as MOAT-C and MRP5), a member of the ABC family of proteins, has anion transporter activity but does not confer multidrug resistance when overexpressed in human embryonic kidney 293 cells, J. Biol. Chem. 274 (1999) 23541–23548.
[34] S. McDonough, N. Davidson, H.A. Lester, N.A. McCarty, Novel pore-lining residues in CFTR that govern permeation and open-channel block, Neuron 13 (1994) 623–634.
[35] H.E. Meyer Zu Schwabedissen, M. Grube, B. Heydrich, K. Linnemann, C. Fusch, H.K. Kroemer, G. Jedlitschky, Expression, localization, and function of MRP5 (ABCC5), a transporter for cyclic nucleotides, in human placenta and cultured human trophoblasts: effects of gestational age and cellular differentiation, Am. J. Pathol. 166 (2005) 39–48.
[36] A.T. Nies, G. Jedlitschky, J. Konig, C. Herold-Mende, H.H. Steiner, H.P. Schmitt, D. Keppler, Expression and immunolocalization of the multidrug resistance proteins, MRP1–MRP6 (ABCC1–ABCC6), in human brain, Neuroscience 129 (2004) 349–360.
[37] A.T. Nies, H. Spring, W.F. Thon, D. Keppler, G. Jedlitschky, Immunolocalization of multidrug resistance protein 5 in the human genitourinary system, J. Urol. 167 (2002) 2271–2275.
[38] S. Pratt, R.L. Shepard, R.A. Kandasamy, P.A. Johnston, W. Perry III, A.H. Dantzig, The multidrug resistance protein 5 (ABCC5) confers resistance to 5-fluorouracil and transports its monophosphorylated metabolites, Mol. Cancer Ther. 4 (2005) 855–863.
[39] A.W. Ravna, I. Sylte, G. Sager, Molecular model of the outward facing state of the human P-glycoprotein (ABCB1), and comparison to a model of the human MRP5 (ABCC5), Theor. Biol. Med. Model. 4 (2007) 33.
[40] G. Reid, P. Wielinga, N. Zelcer, M. de Haas, L. van Deemter, J. Wijnholds, J. Balzarini, P. Borst, Characterization of the transport of nucleoside analog drugs by the human multidrug resistance proteins MRP4 and MRP5, Mol. Pharmacol. 63 (2003) 1094–1103.
[41] C.A. Ritter, G. Jedlitschky, H.E. Meyer Zu Schwabedissen, M. Grube, K. Kock, H.K. Kroemer, Cellular export of drugs and signaling molecules by the ATP-binding cassette transporters MRP4 (ABCC4) and MRP5 (ABCC5), Drug Metab. Rev. 37 (2005) 253–278.
[42] B. Rost, PHD: predicting one-dimensional protein structure by profile-based neural networks, Methods Enzymol. 266 (1996) 525–539.
[43] G. Sager, Cyclic GMP transporters, Neurochem. Int. 45 (2004) 865–873.
[44] M.H. Saier Jr., A functional-phylogenetic classification system for transmembrane solute transporters, Microbiol. Mol. Biol. Rev. 64 (2000) 354–411.
[45] A.E. Senior, D.C. Gadsby, ATP hydrolysis cycles and mechanism in P-glycoprotein and CFTR, Semin. Cancer Biol. 8 (1997) 143–150.
[46] D.N. Sheppard, D.P. Rich, L.S. Ostedgaard, R.J. Gregory, A.E. Smith, M.J. Welsh, Mutations in CFTR associated with mild-disease-form Cl^- channels with altered pore properties, Nature 362 (1993) 160–164.
[47] T. Suzuki, H. Sasaki, H.J. Kuh, M. Agui, Y. Tatsumi, S. Tanabe, M. Terada, N. Saijo, K. Nishio, Detailed structural analysis on both human MRP5 and mouse mrp5 transcripts, Gene 242 (2000) 167–173.
[48] J.A. Tabcharani, J.M. Rommens, Y.X. Hou, X.B. Chang, L.C. Tsui, J.R. Riordan, J.W. Hanrahan, Multi-ion pore behaviour in the CFTR chloride channel, Nature 366 (1993) 79–82.
[49] R.A. van Aubel, P.H. Smeets, J.J. Van Den Heuvel, F.G. Russel, Human organic anion transporter MRP4 (ABCC4) is an efflux pump for the purine end metabolite urate with multiple allosteric substrate binding sites, Am. J. Physiol. Renal Physiol. 288 (2005) F327–F333.
[50] M. Wiederstein, M.J. Sippl, ProSA-web: interactive web service for the recognition of errors in three-dimensional structures of proteins, Nucleic Acids Res. (2007). doi:10.1093/nar/gkm290.
[51] P.R. Wielinga, I. van der Heijden, G. Reid, J.H. Beijnen, J. Wijnholds, P. Borst, Characterization of the MRP4- and MRP5-mediated transport of cyclic nucleotides from intact cells, J. Biol. Chem. 278 (2003) 17664–17671.
[52] J. Wijnholds, C.A. Mol, L. van Deemter, M. de Haas, G.L. Scheffer, F. Baas, J.H. Beijnen, R.J. Scheper, S. Hatse, E. De Clercq,

J. Balzarini, P. Borst, Multidrug-resistance protein 5 is a multispecific organic anion transporter able to transport nucleotide analogs, Proc. Natl. Acad. Sci. U. S. A. 97 (2000) 7476–7481.

[53] W.N. Zagotta, N.B. Olivier, K.D. Black, E.C. Young, R. Olson, E. Gouaux, Structural basis for modulation and agonist specificity of HCN pacemaker channels, Nature 425 (2003) 200–205.

[54] D.W. Zhang, K. Nunoya, M. Vasa, H.M. Gu, A. Theis, S.P. Cole, R.G. Deeley, Transmembrane helix 11 of multidrug resistance protein 1 (MRP1/ABCC1): identification of polar amino acids important for substrate specificity and binding of ATP at nucleotide binding domain 1, Biochemistry 43 (2004) 9413–9425.

[55] K.Y. Zhang, G.L. Card, Y. Suzuki, D.R. Artis, D. Fong, S. Gillette, D. Hsieh, J. Neiman, B.L. West, C. Zhang, M.V. Milburn, S.H. Kim, J. Schlessinger, G. Bollag, A glutamine switch mechanism for nucleotide selectivity by phosphodiesterases, Mol. Cell 15 (2004) 279–286.

[56] J.K. Zolnerciks, C. Wooding, K.J. Linton, Evidence for a Sav1866-like architecture for the human multidrug transporter P-glycoprotein, FASEB J. (2007).